Ecotoxicology and Environmental Safety 266 (2023) 115555

Contents lists available at ScienceDirect

Ecotoxicology and Environmental Safety

journal homepage: www.elsevier.com/locate/ecoenv

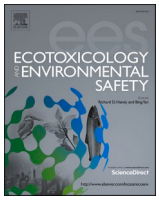

Downregulation of TAZ elicits a mitochondrial redox imbalance and ferroptosis in lung epithelial cells exposed to diesel exhaust particles

Kang-Yun Lee [a,b,1], Ching-Chieh Yang [c,d,1], Pei-Wei Shueng [e,f], Sheng-Min Wu [a], Chih-Hsuan Chen [g], Yi-Chun Chao [g], Yu-Chu Chang [g], Chia-Li Han [h], Hsiao-Chi Chuang [i], Chi-Ching Lee [j], Cheng-Wei Lin [g,k,l,*]

[a] Division of Pulmonary Medicine, Department of Internal Medicine, School of Medicine, College of Medicine, Taipei Medical University, Taipei, Taiwan
[b] Division of Pulmonary Medicine, Department of Internal Medicine, Shuang Ho Hospital, Taipei Medical University, New Taipei City, Taiwan
[c] Division of Radiation Oncology, Chi Mei Medical Center, Tainan, Taiwan
[d] Department of Pharmacy, Chia-Nan University of Pharmacy and Science, Tainan, Taiwan
[e] Division of Radiation Oncology, Far Eastern Memorial Hospital, New Taipei City, Taiwan
[f] Faculty of Medicine, School of Medicine, National Yang Ming Chiao Tung University, Taipei, Taiwan
[g] Department of Biochemistry and Molecular Cell Biology, School of Medicine, College of Medicine, Taipei Medical University, Taipei, Taiwan
[h] Master Program in Clinical Genomics and Proteomics, College of Pharmacy, Taipei Medical University, Taipei, Taiwan
[i] School of Respiratory Therapy, College of Medicine, Taipei Medical University, Taipei, Taiwan
[j] Istanbul Sabahattin Zaim University, Faculty of Engineering and Natural Sciences, Department of Food Engineering, Istanbul, Turkey
[k] Cell Physiology and Molecular Image Research Center, Wan Fang Hospital, Taipei Medical University, Taipei, Taiwan
[l] Drug Development and Value Creation Research Center, Kaohsiung Medical University, Kaohsiung, Taiwan

ARTICLE INFO

Editor: Professor Bing Yan

Keywords:
Ferroptosis
COPD
Particular matter
Mitochondrial redox
Hippo

ABSTRACT

Mitochondrial dysfunction was reported to be involved in the development of lung diseases including chronic obstructive pulmonary disease (COPD). However, molecular regulation underlying metabolic disorders in the airway epithelia exposed to air pollution remains unclear. In the present study, lung bronchial epithelial BEAS-2B and alveolar epithelial A549 cells were treated with diesel exhaust particles (DEPs), the primary representative of ambient particle matter. This treatment elicited cell death accompanied by induction of lipid reactive oxygen species (ROS) production and ferroptosis. Lipidomics analyses revealed that DEPs increased glycerophospholipid contents. Accordingly, DEPs upregulated expression of the electron transport chain (ETC) complex and induced mitochondrial ROS production. Mechanistically, DEP exposure downregulated the Hippo transducer transcriptional co-activator with PDZ-binding motif (TAZ), which was further identified to be crucial for the ferroptosis-associated antioxidant system, including glutathione peroxidase 4 (GPX4), the glutamate-cysteine ligase catalytic subunit (GCLC), and glutathione-disulfide reductase (GSR). Moreover, immunohistochemistry confirmed downregulation of GPX4 and upregulation of lipid peroxidation in the bronchial epithelium of COPD patients and Sprague-Dawley rats exposed to air pollution. Finally, proteomics analyses confirmed alterations of ETC-related proteins in bronchoalveolar lavage from COPD patients compared to healthy subjects. Together, our study discovered that involvement of mitochondrial redox dysregulation plays a vital role in pulmonary epithelial cell destruction after exposure to air pollution.

1. Introduction

Epidemiological studies have demonstrated that long-term exposure to ambient air pollution such as gases and toxic particles, including the notorious particulate matter (PM), is positively related to the risk of chronic respiratory diseases including asthma, chronic bronchitis, and chronic obstructive pulmonary disease (COPD). COPD is now the third leading cause of deaths worldwide (Vogelmeier et al., 2017). Symptoms

* Correspondence to: Department of Biochemistry and Molecular Biology, School of Medicine, College of Medicine, Taipei Medical University, 250 Wu-Xing Street, Taipei 11031, Taiwan.
E-mail address: cwlin@tmu.edu.tw (C.-W. Lin).
[1] These authors contribute equally to this study.

https://doi.org/10.1016/j.ecoenv.2023.115555
Received 16 August 2023; Received in revised form 26 September 2023; Accepted 5 October 2023
Available online 12 October 2023

characterizing COPD include progressive airflow obstruction, airway inflammation, and systemic effects or comorbidities. The damage processes of COPD include inflammation and oxidative stress which are produced by high concentrations of free radicals from tobacco smoke and air pollution. Destruction of connective tissues in the lungs leads to emphysema, which further contributes to poor airflow, and ultimately impairs absorption and release of respiratory gases (Agusti et al., 2023; Brightling and Greening, 2019). Another well-known cause of COPD is inflammation triggered by immune cells, resulting in fibroblast proliferation and tissue remodeling (Aghasafari et al., 2019). Exposure to PM, such as PM with an aerodynamic diameter of < 2.5 μm (PM2.5) and PM10, is recognized to be involved in the COPD pathogenesis. After inhalation of PM, it is internalized into lung epithelial cells and alveolar macrophages, resulting in increased oxidative stress and impaired cellular functions (Feng et al., 2016; Gualtieri et al., 2011). Oxidative stress caused by PM2.5 is suspected of coming from three origins: persistent free radicals in PM2.5 (Gehling and Dellinger, 2013), organic chemicals that are absorbed onto PM2.5, and transitional metals in PM2.5 that disrupt cellular enzymes (Montoya-Estrada et al., 2013). Altogether, increased oxidative stress and inflammation are important mechanisms by which PM2.5 reduces pulmonary function and mediates the development, maintenance, and exacerbation of airway obstruction.

Ferroptosis is a novel non-apoptotic type of cell death that plays a complex role in many pathophysiological developments. Ferroptosis is triggered by disrupted iron homeostasis, resulting in excesses reactive oxygen species (ROS) production through the Fenton reaction and further leads to lipid peroxidation. The process of ferroptosis is closely associated with metabolic processes including iron metabolism, lipid metabolism, and amino acid metabolism (Jiang et al., 2021). Additionally, the involvement of mitochondrial respiration by dysregulating glutaminolysis and polyunsaturated fatty acid (FA; PUFA) synthesis in collaboration with excess ROS consequently promotes lipid peroxidation and aggravates ferroptosis (Chen et al., 2021a). The mainstay of ferroptosis control is the glutathione (GSH) peroxidase 4 (GPX4)/GSH system. GPX4 binds to its cofactor, GSH, to reduce peroxidation of lipids. Additionally, reductions of oxidized GSH (GSSG) by glutathione reductase (GSR) and GSH biosynthesis via cysteine-glutamate also play critical roles in ferroptosis control (Chen et al., 2021a). Recent studies found that ferroptosis is closely associated with the development and progression of many lung diseases including acute lung injury, pulmonary ischemia-reperfusion injury, lung cancer, and COPD (Yu et al., 2021). Besides, patients with COPD have a surfactant lipidome permanent and significant alterations that correlate with disease severity (Agudelo et al., 2020). Additionally, PM2.5 induced ferroptosis in endothelial and neuron cells, and was associated with cardiac fibrosis (Hu et al., 2023; Wang and Tang, 2019; Wei et al., 2022). However, the detailed regulatory mechanism underlying diesel exhaust particle (DEP)-mediated ferroptosis in lung epithelial cells remains unclear.

Yes-associated protein (YAP) and its paralogue, transcriptional coactivator with PDZ-binding motif (TAZ), are transducers of the Hippo pathway which participate in organ development and tissue homeostasis. Dysregulation of the YAP/TAZ signaling pathway contributes to the development and progression of chronic lung diseases, including lung fibrosis, asthma, COPD, and lung cancer (Gokey et al., 2021; LaCanna et al., 2019). YAP is ubiquitously expressed by airway structural cells that regulates airway epithelial stem cells and determines epithelial architecture (Isago et al., 2020; Zhao et al., 2014). Additionally, TAZ regulates expression of surfactant protein C in respiratory epithelial cells (Park et al., 2004), which is essential for normal alveolarization. Loss of TAZ in mice led to an emphysematous lung phenotype that is a typical symptom of patients with COPD (Makita et al., 2008; Yeh et al., 2022). However, the literature regarding the role of YAP/TAZ in COPD development remains unclear. YAP/TAZ plays a crucial role in lipid metabolism and cellular redox homeostasis, and it was recently reported to be involved in ferroptosis in cancer cells (Magesh and Cai, 2022; Yang and Chi, 2020).

Ferroptosis is caused by redox-imbalance that can occur through two major pathways. The production of oxidants from mitochondria, and the reduction of antioxidants by either transporter (e.g., decreased cysteine/glutamine uptake) or enzymatic (e.g., inhibition of GPX4/GCLC) signaling. Although studies have reported that PM2.5 triggered ferroptosis in different cell types, the cellular effect and molecular mechanism underlying DEPs on ferroptosis in lung epithelial cells is still unclear. Herein, we found that a mitochondrial redox imbalance plays a critical role in DEP-mediated ferroptosis in lung bronchial and alveolar epithelial cells. We identified that DEPs exposure increases glycerophospholipid content, and that DEPs upregulates electron transport chain (ETC) complex expression accompanied by increased mitochondrial ROS levels. On the other hand, DEPs decreased the glutathione antioxidant system through downregulating TAZ signaling, and as a result, aggravated lipid peroxidation and promoted the ferroptosis process.

2. Materials and methods

2.1. Cell culture and PM exposure

Human bronchial epithelial BEAS-2B and alveolar type II epithelial A549 cells were purchased from American Type Culture Collection (ATCC). Cells were cultured in RPMI1640 media containing 10% heat-inactivated fetal bovine serum (FBS) supplemented with 100 U/ml penicillin, and 100 U/ml streptomycin (Gibco) in a humid incubator with 5% CO_2. DEPs (SRM 2975) of the National Institute of Standards and Technology were obtained from Sigma-Aldrich. *N*-Acetyl-L-cysteine (NAC) was purchased from Sigma-Aldrich. Cycloheximide (CHX), ferrostatin (Fer)−1, MitoTempo, desferrioxamine (DFX), and verteporfin (VP) were purchased from SelleckChem. BEAS-2B and A549 cells (5000 cells/well) were seeded in 96-well plates in complete medium overnight, after which the medium was refreshed with 1% serum. Cells were treated with DEPs (0–100 μg/ml) and specific inhibitors for 48 h. Cells were refreshed with complete medium containing CCK8 (Donjido), and the formazan product was detected in a microplate reader at a 450-nm wavelength. Cell viability is expressed as the percentage of untreated control cells. Accordingly, a live/death assay was performed using calcein AM/ethidium homodimer (EthD)−1 staining (Biotium).

2.2. Lipidomics analysis

A549 cells (8×10^5) were seeded in 10-cm dishes and treated with 50 μg/ml DEPs for 48 h. Cell pellets were extracted with 500 μL of an organic mixture composed of MeOH/methyl tert-butyl ether (MTBE)/$CHCl_3$ (1.33:1:1, v/v). The extract was mixed (900 rpm) for 1 h at room temperature, and the supernatant was collected after centrifuging at 15,000 relative centrifugal force (rcf) for 10 min. The supernatant was evaporated to dryness with a centrifugal evaporator and was reconstituted with 50 μL of $CHCl_3$/methanol/H_2O (60:30:4.5, v/v). The sample was further diluted with isopropyl alcohol (IPA)/acetonitrile (ACN)/H_2O (2:1:1, v/v) to 100 μL and subjected to a liquid chromatography-quadrupole-time of flight mass spectrometric (LC-QTOF MS; SYNAPT G2 HDMS, Waters) analysis. Metabolites were identified by comparing the accurate masses, tandem MS (MS/MS) fragment spectra, and isotopic patterns to the METLIN mass spectral database and Human Metabolome Database (HMDB vers. 4.0), and LipidBlast. A heatmap was generated with MetaboAnalyst 4.0.

2.3. Western blotting

Protein lysates were extracted using RIPA buffer (50 mM Tris-HCl (pH 7.4), 1% Nonidet P-40, 150 mM NaCl, 1 mM EGTA, and 0.025% sodium deoxycholate) supplemented with a protease and phosphatase inhibitor cocktail (Roche Diagnostics) and separated by sodium dodecylsulfate (SDS)-polyacrylamide gel electrophoresis (PAGE). After

Western transfer, membranes were immersed with blocking buffer (3% bovine serum albumin (BSA)/Tris-buffered saline with Tween ($TBST)_{0.1}$) and incubated overnight with indicated antibodies. Antibodies against phospholipid hydroperoxide GPX4 (GTX54095), GSR (GTX114199), and α-tubulin (GTX112141) were obtained from GeneTex. An antibody against TAZ was obtained from Cell Signaling Technology. Antibodies against human mitochondrial OXPHOS (oxidative phosphorylation) complex cocktail (ab110411) and glutamate-cysteine ligase, catalytic subunit (GCLC; ab53179) were obtained from Abcam. Membranes were washed three times with TBST wash buffer and probed with an appropriate horseradish peroxidase-conjugated secondary antibody (Jackson ImmunoResearch). Protein expression was detected by an enhanced chemiluminescence (ECL) system (Millipore). Western blotting was performed at least three times, and representative experiments are shown. Protein band intensities were quantified using ImageJ software, and data are expressed as fold changes relative to the control group.

2.4. Lipid peroxidation and ROS detection

BEAS-2B and A549 cells were seeded onto eight-well chamber slides, treated with DEPs (100 μg/ml) for 24 h, stained with C11-BODIPY 581/591 (ThermoFisher Scientific) for 30 min, and observed under a fluorescent microscope (Zeiss). Lipid reactive oxygen species (ROS) were quantified by flow cytometry. To detect intracellular ROS and mitochondrion-specific superoxide, cells were treated with DEPs for 24 h followed by staining with 2,7-dichlorodihydrofluorescein diacetate (DCFH-DA, Sigma) and mitoSOX™ Superoxide Red (ThermoFisher Scientific). Intracellular ROS and mitochondrial superoxide were quantified by flow cytometry.

2.5. Immunofluorescent (IF) staining

For TAZ immunostaining, cells were seeded onto eight-well chamber slides and treated with DEPs (100 μg/ml) for 24 h. Cells were fixed with 4% paraformaldehyde for 10 min, blocked with 3% BSA/phosphate-buffered saline (PBS)/$TritonX_{100}$ for 1 h, and then incubated with an anti-TAZ antibody (1:200, Cell Signaling Technology) overnight at 4 °C. Slides were washed with PBS followed by incubation with an Alexa Flour 568-conjugated anti-rabbit antibody (1:250) (Thermo Fisher Scientific) and mounted in UltraCruz mounting medium (Santa Cruz Biotechnology).

2.6. Immunohistochemistry (IHC)

Lung tissues from COPD patients (IRB no. N201902021) and Sprague-Dawley rats with whole-body exposure to 6 months air pollution or high-efficiency particulate air (HEPA) (IACUC no LAC-2015–0290) were formalin-fixed and paraffin-embedded on slides in our previous study (Chen et al., 2021b). Paraffin-embedded tissues were deparaffinized, rehydrated with different concentrations of alcohol, and heated in an unmasking solution (Vector Laboratories) to retrieve antigens. Slides were incubated with anti-GPX4 (1:200, GeneTex), and anti-4-hydroxynonenal (4-HNE; 1:200, R&D Systems) primary antibodies overnight at 4 °C and further incubated with the SignalStain Boost IHC detection reagent (Cell Signaling) at room temperature for 1 h. Slides were washed with PBS and stained with the 3,3′-diaminobenzidine (DAB) peroxidase substrate (Vector Laboratories) (Chung et al., 2020).

2.7. Real-time polymerase chain reaction (PCR)

Total RNA was extracted by a GENzolTM TriRNA Pure kit (Geneaid) and reverse-transcribed by M-MLV reverse transcriptase (Promega). cDNA was amplified by GoTaq qPCR Master Mix (Promega) in a StepOne Plus Real-Time PCR system (Applied Biosystems). Results were calculated using the ΔΔCT equation and are expressed as folds of change relative to control samples. Primer sequences were as follows: GSR (forward (F): 5′-TTCCAGAATACCAACGTCAAAGG-3′; reverse (R): 5′-GTTTTCGGCCAGCAGCTATTG-3′), GCLC (F: 5′-GGCACAAGGACGTTCTCAAGT-3′; R: 5′-CAGACAGGACCAACCGGAC-3′), GPX4 (F: 5′-AGTGGATGAAGATCCAACCCAAGG-3′; R: 5′-GGGCCACACACTTGTGGAGCTAGA-3′), and β-actin (F: 5′-AAGTCCCTTGCCATCCTAAAA-3′; R 5′-ATGCTATCACCTCCCCTGTG-3′).

2.8. Statistical analysis

Data are presented as the mean ± standard deviation (SD) of three independent experiments. Statistical significance was determined by an unpaired, two-tailed Student's *t*-test. $^{*}p < 0.05$, $^{**}p < 0.01$, and $^{***}p < 0.001$ were regarded as statistically significant. All statistical analyses were performed using GraphPad Prism 6.0 software.

3. Results

3.1. DEPs induce lipid peroxidation and provoke ferroptosis in lung epithelial cells

To explore the effect of air pollution on airway epithelial cells, bronchial epithelial BEAS-2B cells and alveolar type II epithelial A549 cells were treated with 0–200 μg/ml DEPs for 24 and 48 h. Results of the CCK8 assay showed that DEP exposure dose-dependently reduced viabilities of BEAS-2B and A549 cells (Fig. 1A), and calcein AM/EthD-I staining indicated that treatment with DEPs at 100 μg/ml induced substantial cell death (Fig. 1B). Ferroptosis is a newly understood type of cell death caused by excessive iron accumulation and increased lipid peroxidation, but its involvement in DEPs-elicited cell death is unclear. We next performed BODIPY 581/591 C11 fluorescent staining to determine the amount of lipid peroxides, a key marker in ferroptosis, in BEAS-2B and A549 cells after exposure to 100 μg/ml DEPs. Fluorescent images showed that cellular oxidized lipids had increased by DEPs in both BEAS-2B and A549 cells (Fig. 1C). Consistent results were obtained by a flow cytometric analysis that treatment with DEPs increased lipid peroxidation, whereas this phenomenon was significantly blocked in the presence of the NAC antioxidant (Fig. 1D), suggesting that DEPs-triggered ferroptosis was involved in ROS production. To confirm the involvement of ferroptosis, BEAS-2B and A549 cells were pretreated with two potent inhibitors of ferroptosis of DFX and Fer-1. DFX is an iron chelator that blocks the Fenton reaction, while Fer-1 acts as a radical-trapping antioxidant to terminate lipid peroxidation. Results showed that the reduced cell viability by DEPs was reversed in the presence of DFX and Fer-1 in both BEAS-2B and A549 cells (Fig. 1**E**).

To further characterize the involvement of lipid metabolism in DEP-elicited ferroptosis, A549 cells were treated with DEPs for 48 h and an untargeted lipidomics approach was applied. Multivariate principal component analysis (PCA) score plot was used to determine the main differences in lipidomic data (Fig. 1F), and PCA and heatmap plots showed that lipid contents were apparently altered after exposure to DEPs in A549 cells (Fig. 1G). Moreover, DEP-treated cells exhibited significantly increased glycerophospholipid species including phosphatidylcholine (PC), phosphatidylethanolamine (PE), and cardiolipin (CL), which are main components of cellular membranes (Fig. 1H). Collectively, these data indicated that DEPs induced lipid peroxidation and provoked ferroptosis in airway epithelial cells.

3.2. DEPs upregulate ETC complex expression and mitochondrial ROS production

Because a mitochondrial redox imbalance plays a crucial role in triggering cell death, and the results showed that NAC treatment diminished DEPs-elicited ferroptosis. We next examined the effect of DEPs on intracellular ROS levels. Results of DCFH-DA staining showed

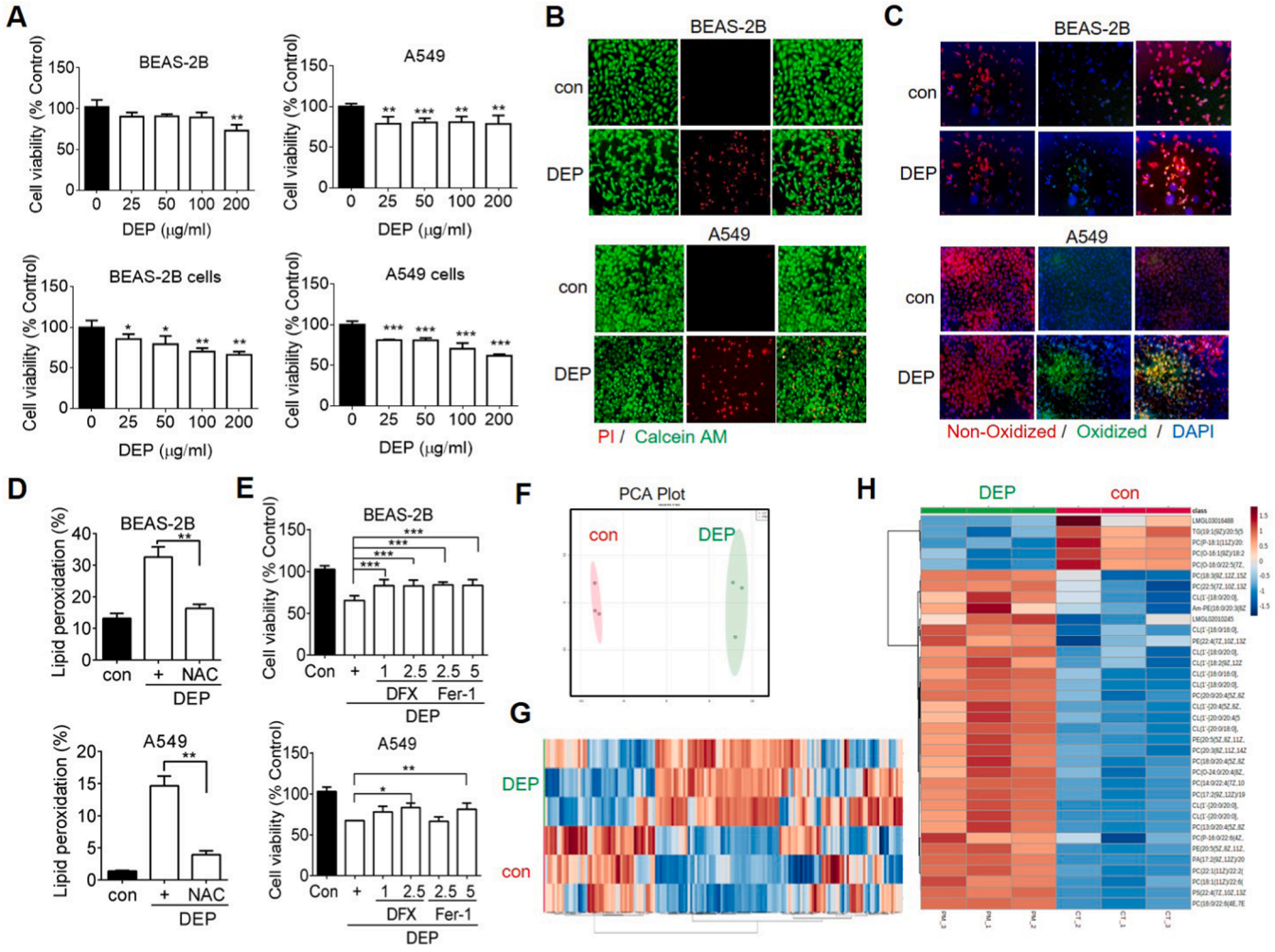

Fig. 1. Diesel exhaust particles (DEPs) induce lipid oxidation and ferroptosis in lung epithelial cells. (A) BEAS-2B and A549 cells were treated with different concentrations of DEPs (0–200 μg/ml) for 24 (upper panel) and 48 h (lower panel), and cell viability was determined by a CCK8 assay. Results are presented as a percentage relative to the control group. Data are expressed as the mean ± SD. Significant differences were analyzed by an unpaired *t*-test, $*p < 0.05$, $**p < 0.01$, $***p < 0.001$. (B) Calcein AM/EthD-1 staining of cell death in BEAS-2B and A549 cells treated with DEPs (100 μg/ml) for 24 h. (C) Representative images of C11-BODIPY 581/591 staining of oxidized lipids in BEAS-2B and A549 cells exposed to DEPs (100 μg/ml) for 24 h. (D) Lipid ROS measurements by C11-BODIPY 581/591 in cells treated with DEPs in the presence or absence of *N*-acetyl-L-cysteine (NAC: 1 mM), and quantification of lipid peroxidation was analyzed by flow cytometry. (E) Suppression of ferroptosis attenuates DEPs-elicited cell death. Cell viability of BEAS-2B and A549 cells treated with DEPs in the presence or absence of deferoxamine (DFX: 1 and 2.5 μM) and ferrostatin-1 (Fer-1: 2.5 and 5 μM) for 48 h. Data are expressed as the mean ± SD. Significant differences were analyzed by an unpaired *t*-test, $*p < 0.05$, $**p < 0.01$, $***p < 0.001$. (F) Score plot of a multivariate principal component analysis (PCA) on lipidomics data from lung epithelial A549 cells exposed to DEPs (50 μg/ml) for 48 h ($n = 3$). (G) Heatmap plots show changes in total and (H) phospholipids from a lipidomic analysis in response to DEPs. Blue, down-expression; red, up-expression.

that DEP treatment significantly increased intracellular ROS levels. Specifically, mitoSOX red staining revealed that DEPs induced mitochondrial superoxide production (Fig. 2A, B). Given that mitochondrial superoxide is mainly produced from the ETC, we next examined the effect of DEPs on the mitochondrial ETC complex. We found that treatment with DEPs increased protein levels of mitochondrial ETC complexes I, II, and III in both BEAS-2B and A549 cells (Fig. 2C), whereas complexes IV and V were not affected by DEPs. These data suggest that DEP-mediated upregulation of the ETC complex may be responsible for mitochondrial superoxide production, which may exacerbate the ferroptotic process. Accordingly, the decreased cell viability, elicited by DEPs, was recovered by pretreatment with NAC or mito-TEMPO, a mitochondria-targeted antioxidant (Fig. 2D). These results support the notion that mitochondrial oxidative stress is involved in DEP-mediated ferroptosis.

3.3. DEPs downregulate TAZ and ferroptosis gene expressions

To further clarify the mechanism underlying DEP-induced ferroptosis in the airway epithelium, we examined the glutathione antioxidant system, which is the mainstay of ferroptosis control. GPX4 functions to interrupt lipid peroxidation using GSH and thus plays a pivotal role in ferroptosis regulation. We found that treatment with DEPs significantly reduced GPX4 protein levels in both BEAS-2B and A549 cells (Fig. 3A). Because GPX4 converts GSH into oxidized glutathione (GSSG), which can be further reduced by GSR, we examined the effect of DEPs on GSR. Intriguingly, the protein level of GSR was suppressed in BEAS-2B but not in A549 cells (Fig. 3A). Moreover, we also examined glutamate-cysteine ligase (GCLC) which is the rate-limiting enzyme for GSH synthesis. Results were similar to those with GPX4 of DEPs suppressing GCLC in BEAS-2B and A549 cells (Fig. 3A). Consistent results were obtained for transcriptional levels of mRNA expressions of GPX4 and GCLC being inhibited by DEPs in BEAS-2B and A549 cells (Fig. 3B). However, the

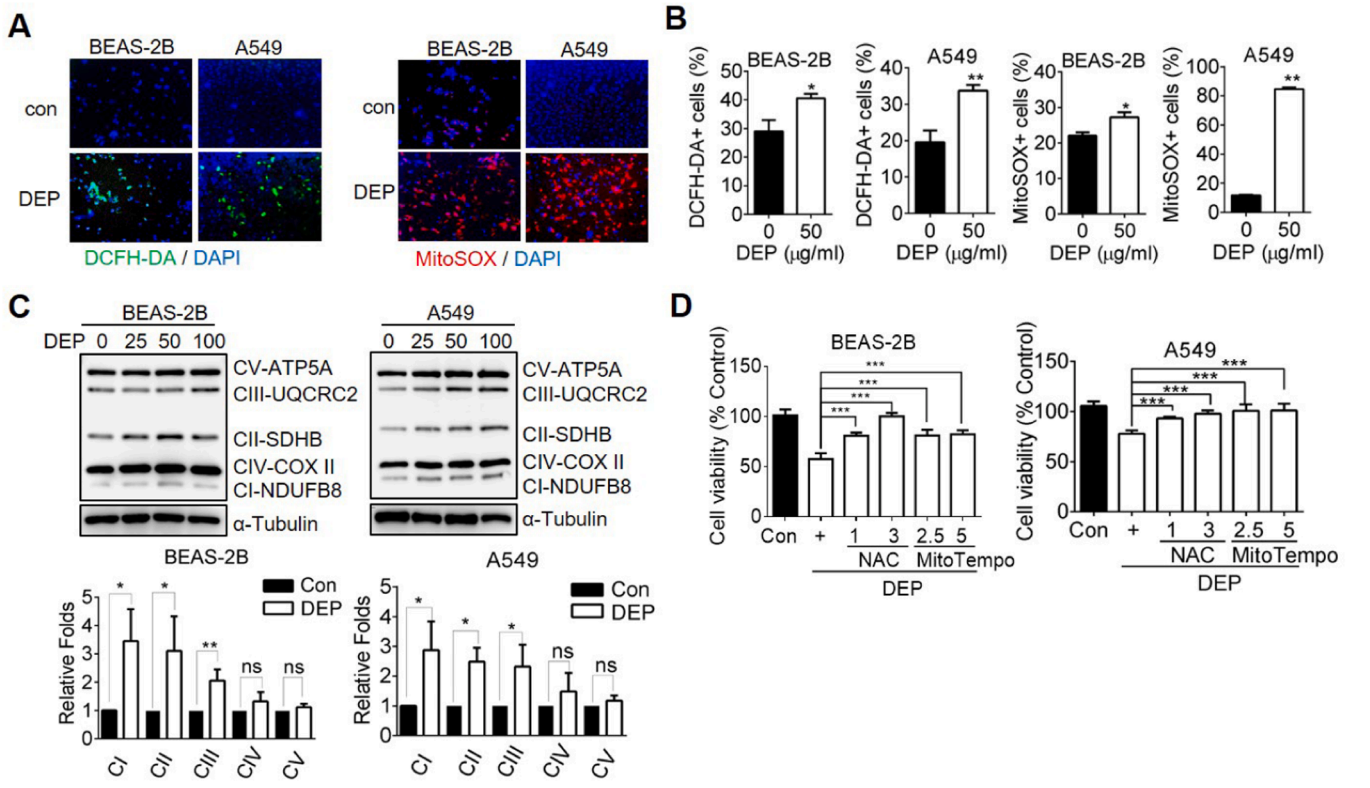

Fig. 2. Diesel exhaust particles (DEPs) upregulate electron transport chain (ETC) complex expression and mitochondrial ROS. (A) Fluorescent images of intracellular ROS (DCFH-DA, left panel) and mitochondrion-specific superoxide (mitoSOX red, right panel) in DEP-treated (100 μg/ml) cells after 24 h of incubation. (B) Intracellular and mitochondrial ROS production was quantified by flow cytometry using DCFH-DA and mitoSOX dyes, respectively. Data were obtained from three independent experiments and are expressed as the mean ± SD. (C) Western blot analysis of ETC proteins from BEAS-2B and A549 cells exposed to DEPs (0–100 μg/ml) for 24 h. Quantification of protein levels was analyzed by ImageJ software. Data were obtained from three independent experiments and are expressed as the mean ± SD. Significant differences were analyzed by an unpaired *t*-test, $*p < 0.05$, $**p < 0.01$, ns, no significance. (D) Cell viability of BEAS-2B and A549 cells exposed to DEPs (100 μg/ml) in the presence of N-acetyl-L-cysteine (NAC; 1 and -3 mM) and MitoTempo (2.5 and 5 μM) for 48 h. Data are expressed as the mean ± SD. Significant differences were analyzed by an unpaired *t*-test, $*p < 0.05$; $**p < 0.01$, $***p < 0.001$.

decreased GSR by DEPs was observed in BEAS-2B but not in A549 cells (Fig. 3A, B).

The Hippo pathway was recently reported to regulate ferroptosis and participated in lipid metabolism; however, its role in DEP-triggered ferroptosis in airway epithelial cells remains unknown. Because we previously identified that the Hippo transducer, TAZ, was upregulated in BEAS-2B and A549 cells (Chao et al., 2021, Lee et al., 2017), we tested the TAZ protein level in response to DEPs. Results of immunofluorescent assay showed that treatment with DEPs decreased the TAZ protein level in nuclei, compared to the control group (Fig. 3C), and treatment with DEP reduced TAZ protein stability in the presence of cycloheximide (Fig. 3D). We also found that the addition of DEPs increased phosphorylation of AMPK in BEAS-2B and A549 cells (Fig. 3E). Given that AMPK is activated by energy dysregulation, and activation of AMPK negatively regulates YAP/TAZ, these data suggested that DEP-mediated mitochondrial dysregulation may contribute to TAZ downregulation in BEAS-2B and A549 cells.

To validate the involvement of the Hippo pathway in ferroptosis, we treated cells with VP, an inhibitor of YAP/TAZ, and results showed that the addition of VP robustly reduced GPX4 and GCLC protein levels in BEAS-2B and A549 cells (Fig. 3F). However, downregulation of GSR by VP was detected in BEAS-2B cells, but not in A549 cells (Fig. 3F). These data were similar to those of DEP treatments, indicating that GSR is regulated in different manners between BEAS-2B and A549 cells.

3.4. Increased lipid peroxidation in airway epithelial cells in rats exposed to air pollution and patients with COPD

To confirm the involvement of ferroptosis in air pollution-elicited pulmonary disorders, we analyzed lung tissues from SD rats with 6 months whole-body exposure to air pollution or high-efficiency particulate air (HEPA) and performed IHC analyses (Chen et al., 2021b). Compared to the control group, we found that rat exposed to air pollution had reduced GPX4 expression in bronchial epithelial tissues (Fig. 4A). On the contrary, the expression of 4-HNE, a major α,β-unsaturated aldehyde product of lipid peroxidation, increased in the bronchial epithelia of PM2.5-treated rats (Fig. 4A). Moreover, patients with COPD exhibited decreased GPX4, accompanied by increased 4-HNE in lung tissues, compared to those in non-COPD patients (Fig. 4B). Moreover, we analyzed GPX4 expression from other COPD cohort (GSE57148) which included 97 COPD subjects and 90 subjects with normal spirometry, and the results were consistent with our findings that GPX4 expression was significantly downregulated in COPD patients (Fig. 4C).

We further analyzed protein changes from bronchoalveolar lavage fluid of COPD patients and healthy subjects using proteomic analyses, and differentially expressed proteins were further analyzed by an Ingenuity pathway analysis (IPA). Consistently, results showed that ETC complex-associated proteins were upregulated in COPD patients (Fig. 5A, B). Collectively, these finding support the notion that aberrant mitochondrial redox is associated with COPD.

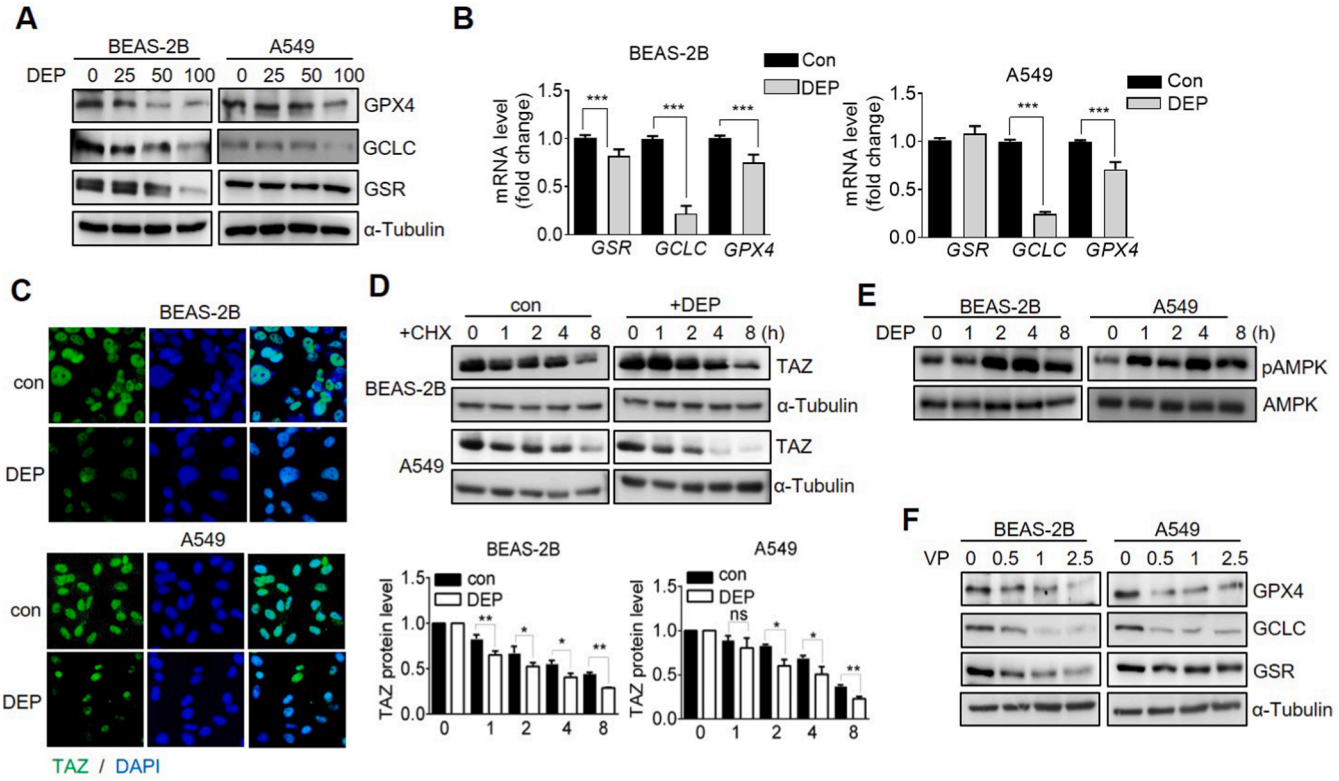

Fig. 3. Diesel exhaust particles (DEPs) downregulate transcriptional co-activator with PDZ-binding motif (TAZ) and ferroptosis gene expressions. (A) Cell lysates from BEAS-2B and A549 cells exposed to DEPs (0–100 μg/ml) for 24 h and protein levels of GSR, GCLC, and GPX4 were measured by a Western blot analysis. (B) Real-time PCR analysis of GSR, GCLC, and GPX4 mRNA expressions in DEP-treated cells. Significant differences were analyzed by an unpaired *t*-test, $^{***}p < 0.001$ (C) Immunofluorescent images show the decrease in nuclear TAZ protein levels after treatment with DEPs (100 μg/ml) in BEAS-2B and A549 cells for 24 h. (D) BEAS-2B and A549 cells were pretreated with cycloheximide (CHX: 50 μg/ml) and then with DEPs (100 μg/ml) for 0–8 h, and cell lysates were collected and TAZ protein levels were analyzed by Western blotting. Relative protein changes were analyzed by ImageJ software. Data were obtained from three independent experiments and expressed as the mean ± SD. Significant differences were analyzed by an unpaired *t*-test, $^{*}p < 0.05$, $^{**}p < 0.01$, ns, not significant. (E) BEAS-2B and A549 cells were treated with DEPs (100 μg/ml) for 0–8 h, cell lysates were collected, and phosphorylated and total AMPK protein levels were analyzed by Western blotting. (F) Cell lysates from BEAS-2B and A549 cells exposed to verteporfin (VP: 0-~2.5 μM) for 24 h, and protein levels of GSR, GCLC, and GPX4 were measured by a Western blot analysis.

4. Discussion

Our study demonstrated that DEPs increased oxidants by upregulating ETC expression followed by elevating mitochondrial ROS. Additionally, DEPs upregulated glycerophospholipid and subsequent triggered lipid peroxidation by mitochondrial ROS. On the other hand, DEPs suppressed antioxidant system including GCLC and GPX4 through attenuating TAZ signaling. Thus, these cellular effects converged to aggravate lipid peroxidation and promote ferroptosis. Studies have reported that PM2.5 induced autophagy-dependent ferroptosis which was identified to be associated with neurotoxicity and cardiac fibrosis (Guo et al., 2023; Wei et al., 2022), and PM2.5 promoted pulmonary epithelial cell senescence and ferroptosis by regulating sirtuin3 (Li et al., 2023). Accordingly, PM2.5 induced ferroptosis by activating AMPK signaling in acute lung and nasal epithelial injury (Gu et al., 2023; Yue et al., 2023). Recently, Wang et al. identified that YAP prevented PM2.5-induced pulmonary toxicity by suppressing NLRP3 inflammasome-mediated pyroptosis, and SLC7A11-dependent ferroptosis (Wang et al., 2023). SLC7A11 is a key transporter maintaining GSH homeostasis. They found that silencing of YAP aggravated PM2.5-mediated mitochondrial ROS production and cell damage in mice lung epithelial MLE12 cells. Similarly, Chang et al. found a decrease of Hippo-YAP in alveolar regions of COPD subjects (Chang et al., 2022). Our data were in line with their findings that TAZ participates in anti-ferroptosis of lung epithelial cells. First, we found that DEPs increased the glycerophospholipid content and lipid ROS levels in lung epithelial cells accompanied by downregulation of GPX4 and GCLC. Moreover, a decrease in GPX4 and an increase in the lipid peroxidation marker, 4HNE, were observed in lung tissues from PM2.5-treated rats and COPD patients. Mechanistically, we found that PM2.5 decreased TAZ protein stability and impeded its nuclear translocation. Suppression of TAZ resulted in downregulation of *GPX4* and *GCLC* gene expressions. Although expression of GSR showed a differentially regulatory pattern upon inhibition of TAZ between A549 and BEAS-2B cells. GPX4 and GCLC participate in GSH biosynthesis, and we previously demonstrated that YAP ameliorated lipid peroxidation by regulating a subset of antioxidant genes (Dai et al., 2022). Similarly, YAP ameliorated hair cell injury by upregulating FTL and TFRC to suppress ferroptosis (Niu et al., 2023). Additionally, YAP induces SLC7A11 expression, thus enabling liver cancer cells to overcome sorafenib-induced ferroptosis (Gao et al., 2021). Altogether, these data indicate that YAP/TAZ harnesses an antioxidant mechanism to protect against various oxidative stresses, at least in part by attenuating ferroptosis. On the contrary, our data identified that DEP treatment decreased the TAZ protein as a result of promoting lipid ROS levels and enhancing lung epithelial cell damage.

Mitochondrial redox homeostasis plays a vital role in regulating various cellular functions, and its imbalance was identified to be involved in PM2.5-mediated cell injury, including COPD. The pathogenesis of COPD is associated with airway inflammation, airway epithelial damage, and airway immunity, and all of these are linked to abnormal or excessive mitochondrial ROS production (Belchamber

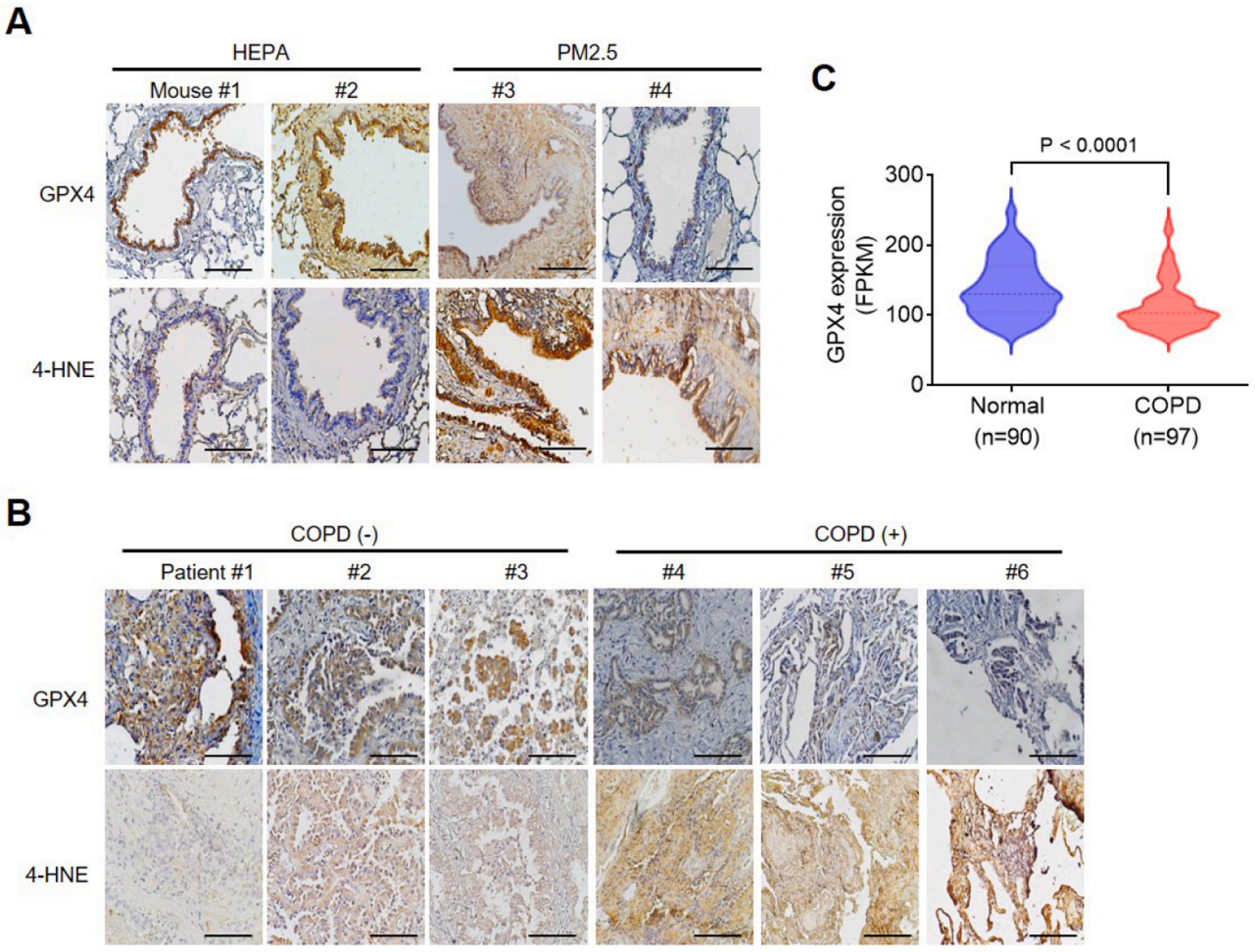

Fig. 4. IHC analyses of ferroptosis in lung tissues from chronic obstructive pulmonary disease (COPD) patients and rats exposed to air pollution. (A) Representative IHC staining of glutathione peroxidase 4 (GPX4) and 4-hydroxynonenal (4-HNE) levels in lung tissues from SD rats with high-efficiency particulate air (HEPA)-filtered and DEP 6 month-exposure groups ($n = 4$ each). Images were taken at 40 × magnification, scale bar= 100 μm. (B) Representative IHC staining of GPX4 and 4-HNE in human lung tissues from COPD subjects and healthy subjects ($n = 5$ each). Scale bar= 100 μm. (C) Violin plot of GPX4 expression level in normal (n = 90) and COPD (n = 97) subjects. Statistical p value was analyzed by unpaired *t*-test.

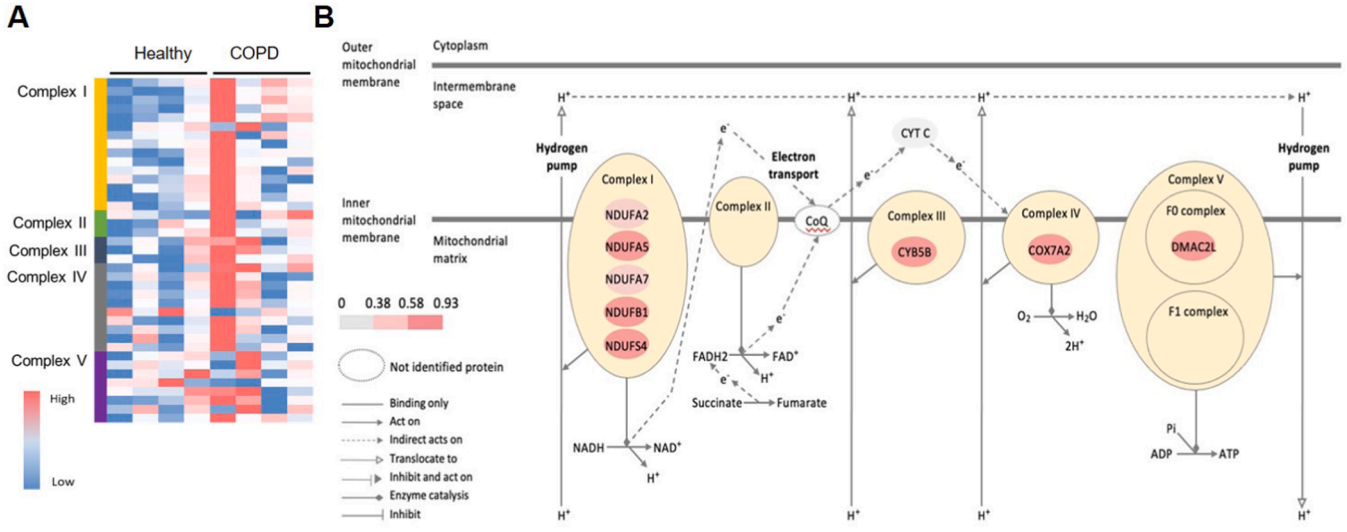

Fig. 5. Proteomics analysis indicates upregulation of electron transport chain (ETC) complex in chronic obstructive pulmonary disease (COPD) patients. (A) Heatmap of results of the proteomics analysis of changes in ETC-related proteins from healthy donors ($n = 4$) and COPD subjects ($n = 4$). Blue, low expression; red, high expression. (B) Ingenuity pathway analysis (IPA) depicts the differentially expressed ETC proteins in COPD patients.

et al., 2019; Frankenberg Garcia et al., 2022; Liu et al., 2023). PM2.5 promotes pulmonary fibrosis by mitochondrial fragmentation and dysfunction (Chang et al., 2023), and PM2.5 promotes vascular fibrosis by targeting the mitochondrial antioxidant, MitoQ (Ning et al., 2021). A PM2.5-mediated NOX4-Nrf2 redox imbalance triggered excessive mitophagy and mitochondrial dysfunction in COPD mice with acute exacerbation (Fan et al., 2023). Moreover, Yue et al. reported that DEPs induced mitochondrial ROS to further induce activation of AMPK and ferritinophagy, and thus exacerbate pulmonary fibrosis (Yue et al., 2023). In the present study, we identified that DEPs increased mitochondrial ETC complexes I, II, and III, accompanied by increased mitochondrial ROS levels in lung epithelial cells. Specific inhibition of mitochondrial ROS rescued DEP-mediated cell death. Moreover, our proteomic analysis supported the notion that ETC complex proteins inclined in COPD patients. These data indicate that upregulation of the ETC complex may be responsible for mitochondrial superoxide production, which may exacerbate the ferroptotic process in DEP-elicited lung cell injury and COPD development.

A549 and BEAS-2B are alveolar and bronchial epithelial cell lines, respectively. Although they are commonly used for in vitro assessment of oxidative stress and cytotoxicity following exposure to air pollutants, differential responses to inflammatory stimuli or hazard material in these two cells were reported. Our data showed that DEPs treatment induced mitochondrial oxidative stress and ferroptosis in both A549 and BEAS-2B cells, but the underlying molecular mechanism showed some discrepancies in response to DEPs. We found that DEPs treatment downregulated GCLC and GPX4 expressions in A549 and BEAS-2B cells; while GSR expression was suppressed in BEAS-2B, but not in A549 cells. Accordingly, our present study applied the two immortalized cells to investigate cellular response in conventional monoculture, it is limited to recapitulate better physiological conditions for respiratory function and structure in a simple environment. Thus, application of 3D culture systems including air-liquid interface polarized airway epithelial model or organotypic culture in primary airway epithelial cells would provide greater physiological relevance and invaluable information on the understanding of specific conditions in COPD pathogenesis.

Conclusion

In summary, we identified an increase in the ETC complex followed by elevation of mitochondrial ROS and downregulation of TAZ-mediated antioxidant capacity that were elicited by DEPs, which exacerbated lipid peroxidation and thus promoted ferroptosis and caused lung epithelial damage. This study shed light for the first time on downregulation of TAZ/GPX4 in lung epithelial injury induced by DEPs, and that also supports the notion of aberrant mitochondrial redox-mediated ferroptosis in the pathogenesis of COPD.

CRediT authorship contribution statement

Kang-Yun Lee, **Ching-Chieh Yang**, **Pei-Wei Shueng**, and **Sheng-Min Wu** conceived and designed research. **Chih-Hsuan Chen**, **Yi-Chun Chao**, **Yu-Chu Chang**, **Chia-Li Han**, **Hsiao-Chi Chuang**, and **Chi-Ching Lee** conducted experiments and analyzed data. **Kang-Yun Lee**, **Ching-Chieh Yang**, and **Pei-Wei Sheung** provided Funding acquisition and Project administration. **Kang-Yun Lee** and **Cheng-Wei Lin** supervised the research. **Cheng-Wei Lin** wrote and revised the paper.

Declaration of Competing Interest

The authors declare that they have no known competing financial interests or personal relationships that could have appeared to influence the work reported in this paper.

Data availability

The authors do not have permission to share data.

Acknowledgements

The authors acknowledge the TMU Core Facility for technical support in the lipidomics analysis. This study was supported by grants from the Ministry of Science and Technology, Taiwan (MOST111-2314-B-038-081, MOST111-2320-B-038-019, and NSTC112-2314-B-038-015 to CWL), Taipei Medical University (DP2-111-21121-01-T-01-04 to CWL), Shuang Ho Hospital (111TMU-SHH-03 to KYL), and Far Eastern Memorial Hospital (FEHM-2021-C-064 and FEHM-2023-C-034 to PWS).

References

Aghasafari, P., et al., 2019. A review of inflammatory mechanism in airway diseases. Inflamm. Res. 68, 59–74.
Agudelo, C.W., et al., 2020. Decreased surfactant lipids correlate with lung function in chronic obstructive pulmonary disease (COPD). PLoS One 15, e0228279.
Agusti, A., et al., 2023. Global Initiative for Chronic Obstructive Lung Disease 2023 Report: GOLD Executive Summary. Eur. Respir. J. 61.
Belchamber, K.B.R., et al., 2019. Defective bacterial phagocytosis is associated with dysfunctional mitochondria in COPD macrophages. Eur. Respir. J. 54.
Brightling, C., Greening, N., 2019. Airway inflammation in COPD: progress to precision medicine. Eur. Respir. J. 54.
Chang, E.M., et al., 2023. PM(2.5) promotes pulmonary fibrosis by mitochondrial dysfunction. Environ. Toxicol. 38, 1905–1913.
Chang, J.H., et al., 2022. Air pollution-regulated E-cadherin mediates contact inhibition of proliferation via the hippo signaling pathways in emphysema. Chem. Biol. Inter. 351, 109763.
Chao, Y.C., et al., 2021. Melatonin downregulates PD-L1 expression and modulates tumor immunity in KRAS-mutant non-small cell lung cancer. Int. J. Mol. Sci. 22.
Chen, X., et al., 2021a. Ferroptosis: machinery and regulation. Autophagy 17, 2054–2081.
Chen, X.Y., et al., 2021b. Alveolar epithelial inter-alpha-trypsin inhibitor heavy chain 4 deficiency associated with senescence-regulated apoptosis by air pollution. Environ. Pollut. 278, 116863.
Chung, C.H., et al., 2020. Fucoidan-based, tumor-activated nanoplatform for overcoming hypoxia and enhancing photodynamic therapy and antitumor immunity. Biomaterials 257, 120227.
Dai, J.Z., et al., 2022. YAP dictates mitochondrial redox homeostasis to facilitate obesity-associated breast cancer progression. Adv. Sci. 9, e2103687.
Fan, X., et al., 2023. PM2.5 increases susceptibility to acute exacerbation of COPD via NOX4/Nrf2 redox imbalance-mediated mitophagy. Redox. Biol. 59, 102587.
Feng, S., et al., 2016. The health effects of ambient PM2.5 and potential mechanisms. Ecotoxicol. Environ. Saf. 128, 67–74.
Frankenberg Garcia, J., et al., 2022. Mitochondrial transfer regulates bioenergetics in healthy and chronic obstructive pulmonary disease airway smooth muscle. Am. J. Respir. Cell Mol. Biol. 67, 471–481.
Gao, R., et al., 2021. YAP/TAZ and ATF4 drive resistance to Sorafenib in hepatocellular carcinoma by preventing ferroptosis. EMBO Mol. Med. 13, e14351.
Gehling, W., Dellinger, B., 2013. Environmentally persistent free radicals and their lifetimes in PM2.5. Environ. Sci. Technol. 47, 8172–8178.
Gokey, J.J., et al., 2021. The role of Hippo/YAP signaling in alveolar repair and pulmonary fibrosis. Front. Med. (Lausanne) 8, 752316.
Gu, W., et al., 2023. Ferroptosis is involved in PM2.5-induced acute nasal epithelial injury via AMPK-mediated autophagy. Int. Immunopharmacol. 115, 109658.
Gualtieri, M., et al., 2011. Airborne urban particles (Milan winter-PM2.5) cause mitotic arrest and cell death: effects on DNA, mitochondria, AhR binding and spindle organization. Mutat. Res. 713, 18–31.
Guo, C.C., et al., 2023. PM(2.5) induces autophagy-dependent ferroptosis by endoplasmic reticulum stress in SH-SY5Y cells. J. Appl. Toxicol. 43, 1013–1025.
Hu, H., et al., 2023. Mechanism of YY1 mediating autophagy dependent ferroptosis in PM2.5 induced cardiac fibrosis. Chemosphere 315, 137749.
Isago, H., et al., 2020. Epithelial expression of YAP and TAZ is sequentially required in lung development. Am. J. Respir. Cell Mol. Biol. 62, 256–266.
Jiang, X., et al., 2021. Ferroptosis: mechanisms biology and role in disease. Nat. Rev. Mol. Cell Biol. 22, 266–282.
LaCanna, R., et al., 2019. Yap/Taz regulate alveolar regeneration and resolution of lung inflammation. J. Clin. Investig. 129, 2107–2122.
Lee, W.Y., Chen, P.C., Wu, W.S., Wu, H.C., Lan, C.H., Huang, Y.H., Cheng, C.H., Chen, K. C., Lin, C.W., 2017. Panobinostat sensitizes KRAS-mutant non-small-cell lung cancer to gefitinib by targeting TAZ. Int J Cancer 141 (9), 1921–1931. https://doi.org/10.1002/ijc.30888.
Li, N., et al., 2023. PM2.5 contributed to pulmonary epithelial senescence and ferroptosis by regulating USP3-SIRT3-P53 axis. Free Radic. Biol. Med. 205, 291–304.
Liu, J., et al., 2023. Mitochondrial quality control in lung diseases: current research and future directions. Front. Physiol. 14, 1236651.
Magesh, S., Cai, D., 2022. Roles of YAP/TAZ in ferroptosis. Trends Cell Biol. 32, 729–732.

Makita, R., et al., 2008. Multiple renal cysts, urinary concentration defects, and pulmonary emphysematous changes in mice lacking TAZ. Am. J. Physiol. Ren. Physiol. 294, F542–F553.
Montoya-Estrada, A., et al., 2013. Urban PM2.5 activates GAPDH and induces RBC damage in COPD patients. Front. Biosci. 5, 638–649.
Ning, R., et al., 2021. The mitochondria-targeted antioxidant MitoQ attenuated PM(2.5)-induced vascular fibrosis via regulating mitophagy. Redox. Biol. 46, 102113.
Niu, X., et al., 2023. Regulation of Hippo/YAP signaling pathway ameliorates cochlear hair cell injury by regulating ferroptosis. Tissue Cell 82, 102051.
Park, K.S., et al., 2004. TAZ interacts with TTF-1 and regulates expression of surfactant protein-C. J. Biol. Chem. 279, 17384–17390.
Vogelmeier, C.F., et al., 2017. Global strategy for the diagnosis, management, and prevention of chronic obstructive lung disease 2017 report. GOLD executive summary. Am. J. Respir. Crit. Care Med. 195, 557–582.
Wang, Y., et al., 2023. YAP1 protects against PM2.5-induced lung toxicity by suppressing pyroptosis and ferroptosis. Ecotoxicol. Environ. Saf. 253, 114708.
Wang, Y., Tang, M., 2019. PM2.5 induces ferroptosis in human endothelial cells through iron overload and redox imbalance. Environ. Pollut. 254, 112937.
Wei, M., et al., 2022. PM2.5 exposure triggers cell death through lysosomal membrane permeabilization and leads to ferroptosis insensitivity via the autophagy dysfunction/p62-KEAP1-NRF2 activation in neuronal cells. Ecotoxicol. Environ. Saf. 248, 114333.
Yang, W.H., Chi, J.T., 2020. Hippo pathway effectors YAP/TAZ as novel determinants of ferroptosis. Mol. Cell Oncol. 7, 1699375.
Yeh, L.Y., et al., 2022. A potent histone deacetylase inhibitor MPT0E028 mitigates emphysema severity via components of the hippo signaling pathway in an emphysematous mouse model. Front. Med. (Lausanne) 9, 794025.
Yu, S., et al., 2021. Recent progress of ferroptosis in lung diseases. Front. Cell Dev. Biol. 9, 789517.
Yue, D., et al., 2023. Diesel exhaust PM2.5 greatly deteriorates fibrosis process in pre-existing pulmonary fibrosis via ferroptosis. Environ. Int. 171, 107706.
Zhao, R., et al., 2014. Yap tunes airway epithelial size and architecture by regulating the identity maintenance and self-renewal of stem cells. Dev. Cell 30, 151–165.